fishes

IMPACT FACTOR 2.4

CITESCORE 3.0

Article

Stock Structure of the Gulf Hake *Urophycis cirrata* (Teleostei: Phycidae) in South-Western Atlantic Using Otolith Shape and Elemental Analyses

César Santificetur, Carmen Lúcia Del Bianco Rossi-Wongtschowski, André Ruperti, Agostinho Almeida, Edgar Pinto and Alberto Teodorico Correia

MDPI

https://doi.org/10.3390/fishes10020063

fishes

MDPI

Article

Stock Structure of the Gulf Hake *Urophycis cirrata* (Teleostei: Phycidae) in South-Western Atlantic Using Otolith Shape and Elemental Analyses

César Santificetur [1,2], Carmen Lúcia Del Bianco Rossi-Wongtschowski [1], André Ruperti [2], Agostinho Almeida [3], Edgar Pinto [4] and Alberto Teodorico Correia [2,5,*]

1 Laboratório de Diversidade, Ecología e Evolução de Peixes—DEEP Lab, Instituto Oceanográfico da Universidade de São Paulo (IOUSP), Praça do Oceanográfico 191, São Paulo 05508-120, Brazil
2 Centro Interdisciplinar de Investigação Marinha e Ambiental (CIIMAR), Avenida General Norton de Matos SN, 4550-208 Matosinhos, Portugal
3 REQUIMTE/LAQV, Laboratório de Química Aplicada, Faculdade de Farmácia da Universidade do Porto (FFUP), Rua Jorge Viterbo Ferreira 228, 4050-313 Porto, Portugal
4 REQUIMTE/LAQV, Escola Superior de Saúde, Instituto Politécnico do Porto, Rua Dr. António Bernardino de Almeida 400, 4200-072 Porto, Portugal
5 Departamento de Produção Aquática, Instituto de Ciências Biomédicas Abel Salazar da Universidade do Porto (ICBAS-UP), Rua Jorge Viterbo Ferreira 228, 4050-313 Porto, Portugal
* Correspondence: atcorreia@icbas.up.pt

Abstract: *Urophycis cirrata* is an important demersal fish species targeted by Brazilian industrial fisheries. With high exploitation rates, its stock(s) is(are) currently deemed fully exploited or overexploited. While basic ecological information, such as length at first maturity, exists, knowledge of its population structure is limited. A sub-sample of 90 sagittal otoliths of *U. cirrata* juveniles (300–411 mm total length) collected during the Program for Assessment of the Sustainable Potential of Living Resources in the Exclusive Economic Zone (REVIZEE) in 2001/2002 was analyzed. Samples came from the outer continental shelf and upper slope of the southeast-south Brazilian coast, divided into three regions: northern (Cabo São Tomé to São Sebastião), central (São Sebastião to Cabo Santa Marta Grande), and southern (Cabo Santa Marta Grande to Chuí). Otolith shape (elliptic Fourier descriptors) and elemental (element:Ca) signatures were examined using univariate (ANOVA, Tukey) and multivariate (MANOVA, LDFA) statistical methods. An overall reclassification success rate of 86% was achieved using both signatures. However, individuals from the three regions were not fully separable, indicating a single, albeit not homogeneous, population unit for fisheries management. As fish stocks are dynamic, contemporary studies should be conducted to verify whether this population structure persists.

Keywords: deep-Sea; demersal-benthic fish species; natural tags; population structure

Key Contribution: The study reveals significant regional variations in the otolith shape and chemistry of *Urophycis cirrata*, indicating environmental influences on its population structure. Despite these variations, the findings suggest a single connected population unit, offering critical insights for fisheries management.

check for updates

Academic Editor: Gioele Capillo

Received: 31 December 2024
Revised: 29 January 2025
Accepted: 31 January 2025
Published: 4 February 2025

Citation: Santificetur, C.; Rossi-Wongtschowski, C.L.D.B.; Ruperti, A.; Almeida, A.; Pinto, E.; Correia, A.T. Stock Structure of the Gulf Hake *Urophycis cirrata* (Teleostei: Phycidae) in South-Western Atlantic Using Otolith Shape and Elemental Analyses. *Fishes* **2025**, *10*, 63. https://doi.org/10.3390/fishes10020063

1. Introduction

Urophycis cirrata (Goode & Bean, 1896) is a benthopelagic deep-water fish species widely distributed across the Atlantic Ocean, from the Gulf of Mexico to southern South America, inhabiting depths ranging from 60 to 700 m [1]. This species has often been

misidentified as *Urophycis mystacea* (Miranda Ribeiro, 1903). This species was originally described as being restricted to the southwestern Atlantic, from southern Bahia to the mouth of the Río de la Plata, on the border between Uruguay and Argentina [2–4]. However, morphological analyses [5] and mitochondrial DNA studies [6] have shown that both names refer to the same species. In this study, the nomenclature *U. cirrata* was adopted, although taxonomic issues are not the primary focus of the present research.

Females of *U. cirrata* are larger than males, with one-year-old individuals exhibiting average total lengths (TLs) of 174.0 mm and 193.0 mm, respectively, reflecting a consistent pattern of differential growth between sexes, as reported in previous studies from the same region [7,8]. Although females exhibit slower growth, they reach older ages [7,8]. Individuals can attain a maximum TL of 676 mm [5,9]. Males are more abundant at greater depths, suggesting possible sexual segregation associated with water depth [10]. This body length difference between males and females, with females dominating at larger sizes, has also been observed in other Gadiform species [11–13]. Reproductive data for females, including ovarian development and the gonadosomatic index, indicate that spawning in southeastern and southern Brazil occurs twice a year, with a peak between April and June [14]. The total length at first sexual maturity for females is 420 mm [15], and their diet is primarily composed of shrimp, crabs, and fish [16].

U. cirrata is a commercially important species in southern Brazil, but its population has experienced a decline since 2001, when it became a target species for bottom trawl fleets [15,17]. Currently, its stock is considered vulnerable and overfished, based on exploitation rates [14]. Furthermore, the established minimum catch size (TL: 300 mm) allows for the capture of individuals that have not yet reached sexual maturity, potentially reducing reproductive opportunities and accelerating population decline [18]. Despite its importance, ecological knowledge about *U. cirrata* remains limited, with little information available regarding its population structure, fish movements, and habitat connectivity. In Brazil, this species is primarily fished using bottom gillnets, especially in the southeastern and southern regions [19]. A stock assessment study revealed that the species is moderately to highly vulnerable to fishing, making it crucial to implement sustainable management measures to ensure both the conservation of *U. cirrata* and the long-term viability of associated fishing activities [20].

Otoliths, inert metabolic structures composed of calcium carbonate, have been widely used as natural markers in studies of fish ecology and fisheries management [21–23]. These structures grow continuously throughout a fish's lifespan, incorporating minor and trace elements from the surrounding environment, which allows the inference of environmental characteristics and habitat use patterns over time [23–25]. Moreover, although otolith morphology is highly species-specific, it also exhibits geographic variation influenced by environmental factors and ontogenetic development [23,26,27]. Insights derived from otolith elemental and shape signatures can provide valuable insights into the population dynamics, movement patterns, and habitat connectivity of marine fish, including in the Southwest Atlantic Ocean [28–30]. Furthermore, spatial segregation in the juvenile and adult stages of a congeneric species, *Urophycis brasiliensis*, was successfully studied using otolith microchemistry and shape analyses [31].

This study applies, for the first time, otolith elemental and shape analyses to investigate the population structure of *U. cirrata* along the southeast-south Brazilian coast, from Rio de Janeiro to Santa Catarina. The aim is to provide new insights into its ecological dynamics and support fisheries management and conservation strategies.

2. Materials and Methods

2.1. Biological Sampling

The individuals of *U. cirrata* were collected during research expeditions conducted as part of the Evaluation of the Sustainable Potential of Living Resources Program in the Brazilian Exclusive Economic Zone (REVIZEE) in 2001 (August, September, and October) and 2002 (February, April, and June). This program was coordinated by the Brazilian Institute of the Environment and Renewable Natural Resources (IBAMA) and involved several universities and research institutions. Fish used in this study were collected by research and commercial vessels during the fishing prospecting campaigns [10]. The fish were captured using bottom trawls, circular and rectangular traps (large and small), handlines, droplines and bottom longlines. The sampling area was from Cabo Frio, in Rio de Janeiro (23°05′ S), to Chuí, in Rio Grande do Sul (34°34′ S), at depths of 94 to 810 m (Figure 1). Fish were morphologically identified to the species level [32], preserved on ice and transported to the laboratory. Fish were measured [total length (TL) to the nearest 1 mm], and sagittal otoliths were carefully removed, washed in distilled water, air-dried, and preserved in plastic tubes.

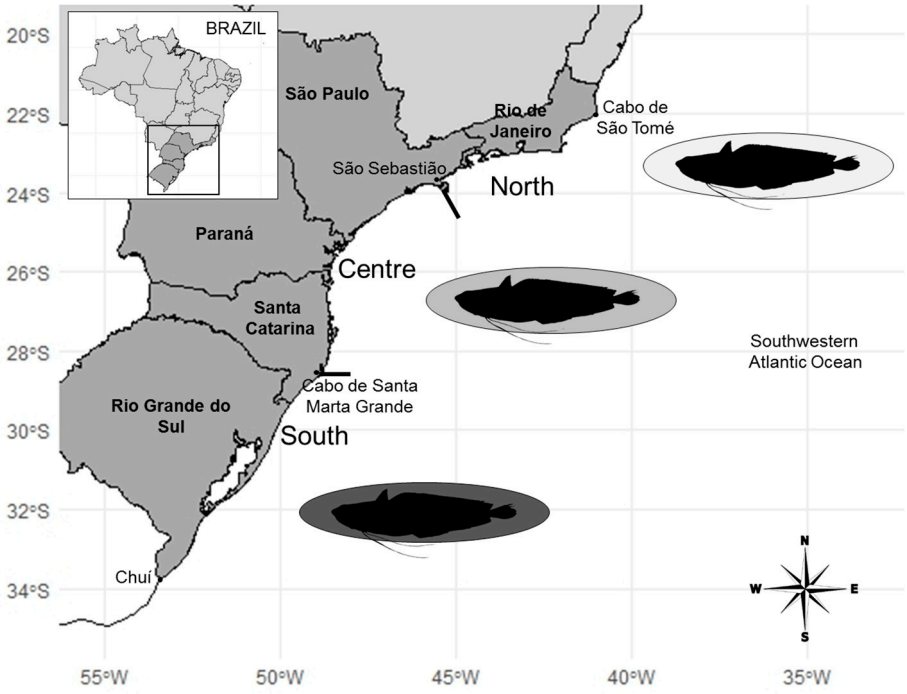

Figure 1. Map of Brazil (inset map) showing the sampling area of *Urophicys cirrata* individuals used in this study (main map) that includes the Brazilian southeastern-south oceanic extension delimited by the geographic coordinates from 23°05′ S–47°21′ W (Cabo de São Tomé, Rio de Janeiro) to 34°34′ S–52°01′ W (Chuí, Rio Grande do Sul).

To minimize any potential confounding effect of regional differences in fish growth on otolith shape and chemistry, an attempt was made to collect individuals from the same age class by choosing fish of similar length [27,28,30]. A sub-sample of 90 (30 per region) individuals of similar length (TL: 300–411 mm (Table 1); One-Way ANOVA: $F_{2,87} = 0.208$ and $p = 0.813$) from southeast-south Brazil, considering the oceanography study area division from the north (Cabo de São Tomé to São Sebastião), center (São Sebastião to Cape of Santa Marta Grande), and south (Cape of Santa Marta Grande to Chuí) [33], was selected.

Table 1. Region, geographic coordinates, sample size (n) and total length (TL: mean ± SD) of the individuals used in this study.

Region	Latitude	Longitude	N	TL (mm)
North	23°05′ S–26°46′ S	042°03′ W–047°21′ W	30	360.43 ± 30.92
Center	28°40′ S–31°07′ S	047°01′ W–049°49′ W	30	357.70 ± 32.59
South	31°07′ S–34°34′ S	047°31′ W–052°01′ W	30	363.00 ± 28.33

2.2. Otolith Shape Analysis

Although left and right otoliths are considered morphologically identical in this species [8], the right otolith was chosen for analysis based on a similar study of the congeneric *U. brasiliensis* [31]. A microphotograph of each right otolith was taken by a stereomicroscope (Meiji Techno, Saitama, Japan, EMZ-13TR) coupled with a USB digital camera (Olympus, Tokyo, Japan, SC30), using reflected light against a dark background. Sagittae were positioned with the sulcus acusticus up, and the rostrum pointed to the left. Orthogonal two-dimensional pictures were thereafter transformed into black and white images using the software Paintnet (version 4.1.6). The final images were processed with the software Shape Analysis v. 1.3 to obtain the Elliptic Fourier Descriptors (EFDs).

The contour shape was extracted [34] from each otolith to determine the number of EFD required to adequately describe its outline [35]. The first five harmonics reached 95% of the cumulative power (excluding coefficient d5). Moreover, since the elliptical Fourier harmonics for each otolith were normalized to the first harmonic and were thus invariant to the otolith size [36], the first three coefficients (a1, b1 and c1) constant for all outlines were excluded, reducing the number of EFD to 16 (i.e., $5 \times 4 - 1 - 3 = 16$).

2.3. Otolith Elemental Analysis

Right sagittal otoliths were cleaned in an ultrasonic bath for 5 min in ultrapure water (H_2O, Milli-Q-Water) to remove any adherent biological tissues, followed by immersion in 3% analytical grade hydrogen peroxide (H_2O_2, Fluka Trace Select) for 15 min, to remove any remaining organic residues. Otoliths were then rinsed in ultrapure 1% nitric acid (HNO_3, Fluka Trace Select) solution for 10 s, followed by a triple-immersion in ultrapure water (H_2O, Milli-Q-Water) for 5 min to remove the acid [37]. Finally, otoliths were stored in pre-cleaned plastic tubes and dried in a laminar flow hood [38]. The decontaminated otoliths were weighed on an analytical balance (OM, 0.0001 g) prior to further analyses.

Sagittae were dissolved for 15 min in 60 µL of ultrapure nitric acid (HNO_3, Fluka Trace Select, >69%), diluted with ultrapure water (H_20, Milli-Q-Water) to a final volume of 3 mL [2% of HNO_3 (v/v) and 0.02% of TDS (m/v)] [30], stirred with a vortex and thereafter sent to analysis. Except for calcium, multi-elemental analysis was performed by Inductively Coupled Plasma Mass Spectrometry (ICP-MS) using an iCAP™ Q instrument (Thermo Fisher Scientific, Bremen, Germany) equipped with a concentric glass nebulizer, a Peltier-cooled baffled cyclonic spray chamber, a standard quartz torch and a two-cone interface design (sample and skimmer nickel cones). High-purity (99.9997%) argon (Gasin II, Leça da Palmeira, Portugal) was used as the nebulizer and plasma gas. The equipment control and data acquisition were made through the Qtegra software (Thermo Fisher Scientific, Bremen, Germany, V2.14). To minimize the effect of plasma fluctuations or different nebulizer aspiration rates among samples, Indium (115In), Scandium (45Sc), Yttrium (89Y) and Terbium (159Tb) were monitored as internal standards. The limits of detection (LODs) were calculated as the concentration corresponding to three times the standard deviation of 10 sample blanks. Calcium was determined by a Flame Atomic Absorption Spectrometry instrument (FAAS) (Perkin Elmer, Überlingen, Germany). Samples were analyzed in random order to avoid possible sequence effects.

The NRC otolith certified reference material FEBS-1 [39] was used for accuracy control with recovery rates > 95%. Precision of replicate analyses of individual elements ranged between 3% and 4% of the relative standard deviation. Eleven elements were above the LOD: 44Ca (0.086 mg/L), 23Na (45.682 µg/L), 88Sr (22.600 µg/L), 7Li (0.037 µg/L), 24Mg (9.424 µg/L), 55Mn (1.494 µg/L), 75As (0.710 µg/L), 85Rb (0.074 µg/L), 82Se (10.542 µg/L), 59Co (0.391 µg/L) and 137Ba (2.768 µg/L). The trace elements' concentrations, originally in µg element/L solution, were transformed into µg element/g otolith and finally into µg element/g calcium [40].

2.4. Statistical Analysis

Although the present study used individuals within the same total-length range (as a proxy of the year class), it was necessary to ensure that differences in fish size among samples did not interfere with the analysis of site-specific variations in otolith chemistry [41]. To address this, the relationships between the elemental ratios (Element:Ca) and fish size were evaluated using analysis of covariance (ANCOVA), with OM as the covariate, prior to conducting further statistical analyses. The results indicated that Mg:Ca and Ba:Ca showed a negative relationship with OM (ANCOVAs, $p < 0.05$). These variables were corrected using the formula $Vadj = V - (\beta \times \text{covariate})$, where Vadj is the adjusted sample value, V is the original sample value, and β is the ANCOVA slope value [42].

The data were checked for normality (Shapiro–Wilk test) and homogeneity of variances (Levene's test). These assumptions were met after a log10 transformation. One-Way Analysis of Variance (One-Way ANOVA) was used to explore regional differences in otolith elemental and shape signatures. ANOVA was followed by a Tukey post-hoc test for significant differences ($p < 0.05$). Multivariate Analyses of Variance (MANOVA) were used to test for regional differences in otolith multi shape and elemental signatures. For MANOVA, the approximate F-ratio statistic for the most robust test of multivariate statistics (Pillai's trace) was reported. Multivariate pairwise comparisons were evaluated using the Hotelling's T-squared test. A Linear Discriminant Function Analysis (LDFA) using the stepwise mode was used to visualize regional differences and to examine the re-classification accuracy of fish to their original location, verified through the percentage of correct re-classification accuracies of the discriminant functions using a jack-knifed matrix [43].

All statistical analyses were performed using Systat (v. 12), PRIMER 6+PERMANOVA and Past 4.03 softwares. A level of significance (α) of 0.05 was used. Data are presented as means ± standard deviations.

3. Results

3.1. Otolith Shape Analysis

Most of the EFD showed no significant differences among regions, with the exception of D1, D2, and A3, which showed significant differences in otolith contours across regions (One-Way ANOVAs, $p < 0.05$) (Table 2). The Tukey tests for D1 showed significant differences between the southern region and the other two regions (Tukey tests, $p < 0.05$) (Table 2). For D2, a significant difference was found only between the Center and North ($p = 0.014$) (Table 2). For A3, the only significant difference was between the North and South ($p = 0.020$) regions (Table 2). These findings were further corroborated by the MANOVA, which confirmed significant regional differences in otolith contours (Pillai's trace, $F = 2.457$, $p < 0.01$). Post-hoc Hotelling's tests ($p < 0.01$) showed significant statistical differences in the southern region compared to the other two regions. The LDFA plot did not clearly distinguish individuals from the three regions, with the center region showing a

significant overlap with the northern and southern regions (Figure 2A). The EFD achieved an overall jack-knifed reclassification rate of 69% (Table 3).

Table 2. Univariate analysis of EFD for *Urophycis cirrata*. Results of the One-Way ANOVAs, including the degrees of freedom (DF), F-statistics (F) and *p*-values (*p*), followed by the pairwise Tukey post-hoc test outcomes, if needed ($p < 0.05$). Regions are represented as N (North), C (Center), and S (South). Bold values represent statistically significant differences.

EFD	ANOVA			Tukey Tests (*p*-Values)		
	DF	**F**	***p***	**N × C**	**N × S**	**C × S**
D1	2.87	12.41	**0.000**	0.419	**0.000**	**0.002**
A2	2.87	1.59	0.210			
B2	2.87	2.01	0.140			
C2	2.87	1.40	0.252			
D2	2.87	4.16	**0.019**	**0.014**	0.234	0.438
A3	2.87	4.03	**0.021**	0.725	**0.020**	0.122
B3	2.87	0.40	0.673			
C3	2.87	0.55	0.580			
D3	2.87	0.15	0.864			
A4	2.87	0.63	0.536			
B4	2.87	1.82	0.168			
C4	2.87	0.55	0.579			
D4	2.87	2.91	0.060			
A5	2.87	2.89	0.061			
B5	2.87	2.49	0.089			
C5	2.87	0.16	0.852			

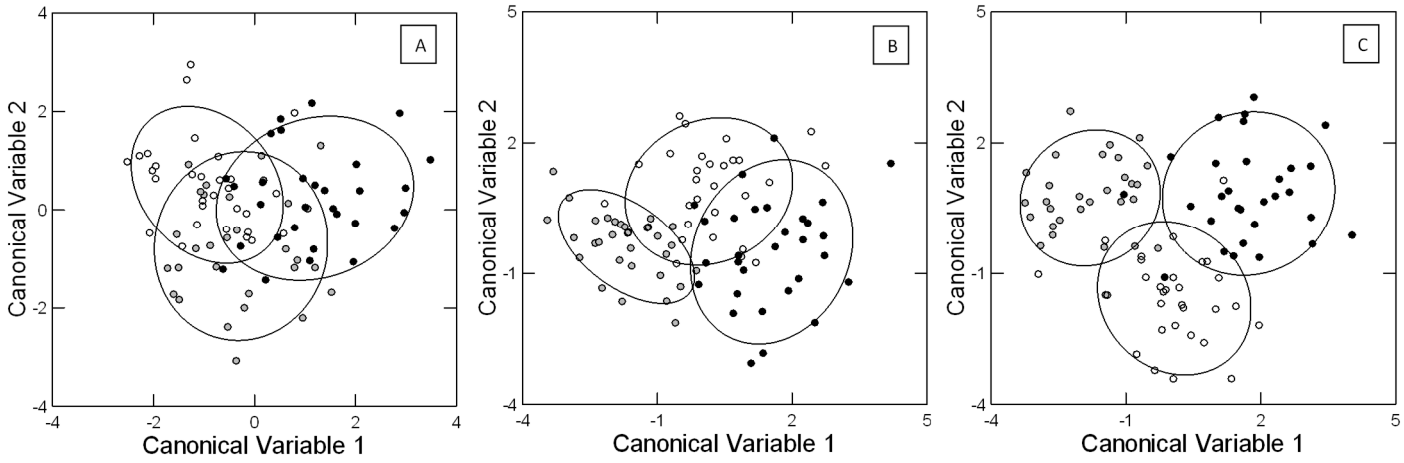

Figure 2. Linear discrimination function analysis plots displaying the spatial differences of *Urophicys cirrata* otoliths using (**A**) shape analysis, (**B**) elemental analysis, and (**C**) all techniques combined from the three sampling regions along the southeast-south Brazilian coast. North (white dot), Center (grey dot) and South (black dot) regions. The ellipses indicate 95% confidence intervals, with overlapping areas highlighting regions with greater similarities in terms of otolith characteristics. The dots represent individual fish.

Table 3. Jackknife re-classification matrix of *Urophicys cirrata* adults obtained from linear discriminant function analysis in stepwise mode of the individuals collected at the three main regions based on the otolith shape analysis (A), otolith elemental analysis (B) and both analyses combined (C).

Real Location	**Predicted Location**			
A	North	Center	South	**%**
North	22	7	1	73
Center	8	19	3	63
South	1	8	21	70
Total	31	31	28	69
B	North	Center	South	**%**
North	19	6	5	63
Center	4	26	0	87
South	5	3	22	73
Total	28	35	327	74
C	North	Center	South	**%**
North	23	6	1	77
Center	1	28	1	93
South	2	3	25	83
Total	26	37	27	84

3.2. Otolith Elemental Analysis

Otolith elemental analyses revealed distinct patterns in element:Ca ratios across the three studied regions (Figure 3). Mn:Ca, Co:Ca, Se:Ca, Li:Ca and Rb:Ca exhibited similar concentrations across regions (One-Way ANOVAs, $p > 0.05$), whereas Na:Ca exhibited significant differences across all regions (One-Way ANOVAs, followed by Tukey tests, $p < 0.05$). Ba:Ca and As:Ca displayed distinct concentrations exclusively in the southern region (higher and lower concentrations for Ba:Ca and As:Ca, respectively) (One-Way ANOVAs, followed by Tukey tests, $p < 0.05$). Mg levels differed between the northern and southern regions, with the center region showing intermediate values (One-Way ANOVA, followed by Tukey tests, $p < 0.05$). Sr exhibited a pattern where the southern region differed from the center region, while the northern region showed similarities with both (One-Way ANOVA, followed by a Tukey test, $p > 0.05$) (Figure 3). The LDFA plot clearly distinguished between the center and southern regions, while the northern region exhibited considerable overlap with the other regions (Figure 2B). The use of the Element: Ca ratios allowed for the achievement of an overall jack-knifed reclassification rate of 74% (Table 3).

3.3. Both Tools Combined

All combined natural otolith markers showed significant statistical differences among regions (MANOVA, Pillai's Trace $p < 0.05$), with all pairwise comparisons showing significant differences (Hotelling's T-square tests $p < 0.05$). The LDFA plot (Figure 2C) did not fully discriminate the regions, showing slight overlap, particularly between the north and center regions. Combining otolith shape and elemental signatures led to an overall reclassification rate of 84% (Table 3).

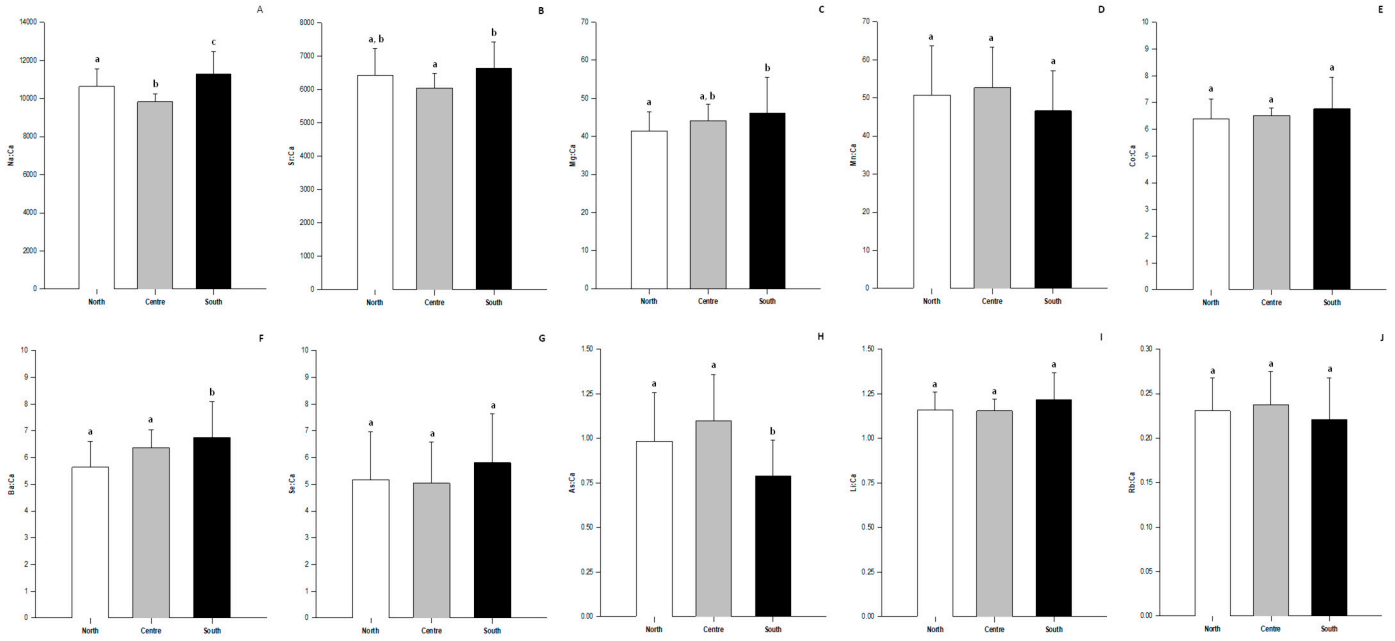

Figure 3. Elemental (detrended for Mg and Ba) concentrations in μg element/g calcium (Mean ± SD) in whole otoliths of *Urophicys cirrata* collected in the southeast-south Brazil for (**A**) Na:Ca, (**B**) Sr:Ca, (**C**) Mg:Ca, (**D**) Mn: Ca, (**E**) Co:Ca, (**F**) Ba:Ca, (**G**) Se:Ca, (**H**) As: Ca, (**I**) Li:Ca and (**J**) Rb:Ca. The regions marked with the different letters are significantly different from each other (One-Way ANOVAs, followed by the Tukey tests, $p < 0.05$).

4. Discussion

The objective of this study was to investigate regional variations in the morphology and chemistry of *Urophycis cirrata* otoliths to better understand the species' population structure through natural markers. Multivariate analysis revealed regional differentiation; however, the overlap in otolith shape and chemical composition data suggests a predominantly connected population. The combined analysis of otolith morphology and elemental composition further emphasized that, while the population remains largely interconnected, regional environmental factors—such as water chemistry, prey availability, and habitat characteristics—partially influence its structure. These findings align with previous studies emphasizing the complementary value of otolith morphometry and microchemistry in understanding the population structure of marine species in this area [28,44,45], reinforcing the effectiveness of these methods in delineating fish populations under varying environmental pressures.

Otolith shape signatures have demonstrated their utility, albeit with certain limitations, in identifying regional differences, achieving an overall reclassification rate of 69%. The morphological analysis revealed significant regional differences, likely reflecting the influence of environmental gradients on otolith morphology. These regional patterns correspond to the dynamic oceanographic characteristics of the southeast-south coastal region of Brazil, where temperature, salinity, and sediment types are shaped by the interaction of distinct water masses. For instance, the warmer, saltier waters of the Brazil Current dominate the continental shelf, while the cooler, less saline waters of the South Atlantic Central Water and the Falkland Current create marked thermal and salinity gradients [46–48].

The sediments in this area exhibit a clear latitudinal transition. The northern region is characterized by sandy and biogenic sediments rich in carbonate, while the southern region has finer sediments, rich in silt and clay, with a higher organic matter content [49]. This pattern reflects the influence of the Brazil Current, which transports biogenic minerals and fine particles from tropical regions, and the Río de la Plata, the primary source of terrigenous

sediments south of 27°S [49–51]. The mineralogical composition further highlights a latitudinal distinction, with illite dominating in the south, derived from the Río de la Plata Basin, and kaolinite prevailing in the north, associated with chemical weathering in tropical environments [51].

Previous studies indicate that otolith shape is influenced by both endogenous factors, such as growth and age, and exogenous factors, such as temperature and salinity, which vary geographically [52–54]. For the same species, a preliminary study using morphometric data and shape indices of otoliths indicated a possible latitudinal variation [55]. Although Elliptic Fourier Descriptors (EFDs) are invariant with respect to otolith size, their sensitivity to subtle variations in contours makes them particularly useful for distinguishing populations exposed to different environmental pressures [35], such as those imposed by the diverse oceanographic conditions in this area. Despite the limitations observed in previous research, EFDs have proven effective in spatial discrimination, even in contexts of high population connectivity, highlighting their utility in identifying regional variations in otolith morphology [44,53,56]. These results emphasize the use of otolith morphometry as a valuable tool for population structure studies, particularly when integrated with other natural tags.

Knowledge about multi-elemental signatures in fish otoliths, particularly the mechanisms underlying the incorporation of minor and trace elements, remains largely restricted to a limited set of elements [57]. In general, these elements are assimilated into the aragonitic matrix through absorption from water via the gills and intestines. Once in the bloodstream, they are transported to the inner ear and pass through the endolymph before being deposited into the otolith matrix [58–60]. The chemical composition of otoliths is shaped by a complex interplay of environmental and physiological factors. Among exogenous factors, water temperature, salinity, feeding regimes, and chemical gradients in the surrounding environment have a direct influence on both otolith chemistry and morphology [44,59,61]. Conversely, the incorporation of minor and trace elements into the aragonite matrix is also modulated by endogenous factors, including interactions with specific structural proteins involved in otolith formation and development [57,60,62].

Elements sourced exclusively from the saline fraction of the endolymph, including 88Sr, 7Li, 11B, 24Mg, 39K, 55Mn, and 138Ba, have demonstrated significant utility in the geographic differentiation of individuals. Since these elements are not protein-bound, they are more likely to reflect the environmental characteristics of their regions of origin directly [57,60,63]. In this study, five of these elements (Sr:Ca, Li:Ca, Mg:Ca, Mn:Ca, and Ba:Ca) were analyzed, along with Co:Ca, Na:Ca, Se:Ca, As:Ca, and Rb:Ca. Among these ten element:Ca ratios, half (e.g., Mn:Ca, Co:Ca, Se:Ca, Li:Ca, and Rb:Ca) did not exhibit statistically significant differences among regions. Conversely, the other five ratios (e.g., Na:Ca, Sr:Ca, Mg:Ca, Ba:Ca, and As:Ca) showed significant regional variation, indicating potential environmental influences on their incorporation into otoliths.

The Ba:Ca ratios in otoliths typically show a negative correlation with water salinity, as barium is primarily introduced into marine environments through riverine inputs. However, this relationship can vary depending on watershed characteristics, particularly in volcanic regions, where Ba concentrations are naturally higher [64–66]. The elevated Ba:Ca values observed in the southern region suggest lower salinity levels, likely influenced by the Brazil-Malvinas Confluence. This dynamic region marks the interaction between the warm and saline Brazil Current and the cold, less saline Malvinas Current, leading to a highly variable oceanographic environment [48,67]. These interactions create sharp gradients in temperature and salinity, which can influence the incorporation of trace elements in otoliths. In contrast, the northern and center regions are predominantly influenced by the Brazil Current, characterized by higher salinity and more stable hydrographic conditions

due to a reduced input from subantarctic waters and minimal freshwater discharge. The northern region is also affected by the South Atlantic Central Water (SACW) and Tropical Water (TW), which dominate at shallower depths, creating distinct vertical stratification layers [46,47]. While U. cirrata is most abundant at depths between 150 and 300 m [14], variations in surface salinity and water mass properties may indirectly affect otolith chemistry through oceanographic processes such as vertical mixing, upwelling, and subsidence, which transport surface characteristics to deeper layers [68,69].

The Sr:Ca ratios in otoliths are generally positively correlated with water salinity and have proven effective in identifying regional differences in hydrographic characteristics in similar studies [56,65,66]. The observed Sr:Ca distribution, where the southern region differs from the center region and the northern region displays values similar to both, reflects the mixing of water masses. This mixing involves the interaction of coastal waters, such as the Brazil Current, with the central South Atlantic waters and contributions from the South Atlantic Central Water (SACW) at depth [47]. These complex mixing processes likely shape the salinity gradients recorded in otoliths. However, the contrasting patterns between Sr:Ca and Ba:Ca suggest that additional environmental or biological factors may also influence the observed variations [70].

The Mg:Ca ratios in otoliths exhibited distinct regional differences, with significant variations between the northern and southern regions, while the center region showed intermediate values, suggesting an environmental gradient. Studies suggest that Mg:Ca in otoliths is positively correlated with temperature, but its incorporation may also be influenced by metabolic processes due to its essential role in tightly regulated cellular functions [71–73]. Higher Mg:Ca concentrations observed may reflect intense metabolic activity during early life stages, particularly in areas with environmentally favorable conditions for productivity [73]. In contrast, lower Mg:Ca concentrations, especially in older individuals, may be linked to reduced metabolic rates as individuals age [29,73].

Arsenic (As), widely recognized as a toxic element, is predominantly of natural origin in the waters of South America, making it one of the main contaminants of public health concern [74–76]. In the southwestern Atlantic, elevated arsenic levels have been reported in both water and fish muscle, reflecting the impacts of bioaccumulation in marine organisms [77–79]. This chemical element is primarily absorbed through diet, a pathway that is more significant than direct absorption from water, except in cases of extremely high aquatic concentrations [80]. Its bioaccumulation can vary with ontogenetic factors such as fish size and age, which influence the rates of arsenic accumulation [81,82]. In the southern region, the lower As:Ca ratio can be attributed to various environmental and ecological factors, such as higher oxygenation and lower concentrations of organic-rich sediments, which reduce arsenic bioavailability [74,80]. Additionally, benthic prey available in this region may have lower arsenic concentrations, limiting its bioaccumulation in fish [77,79]. The reduced influence of anthropogenic sources, such as industrial and agricultural discharges, also contributes to the reduced levels observed in the southern region [78]. Ontogenetic factors, including variations in metabolic rates and growth patterns, can further impact the incorporation of arsenic into otoliths [73].

Similar to other minor elements, sodium (Na) is physiologically regulated and plays a crucial role in metabolic processes, being essential for growth and reproduction in organisms [22,60,83]. However, Na levels found in fish otoliths may reflect geographical and habitat variations, influenced by factors such as the geological characteristics of the waters which the fish inhabit, as well as contamination from human activities in the water masses [54,84,85]. The deposition of Na in otoliths can also be affected by ontogenetic effects during the growth of the fish [86], as well as by stressful events throughout their life [87]. Additionally, the concentration of Na in otoliths may correlate with water salinity,

with higher levels in more saline environments [88]. The interaction of Na with other elements, such as strontium (Sr), should also be considered, as it may influence the incorporation and variation of the Na:Ca ratio in otoliths [89]. The lack of uniformity in Na composition in otoliths, as well as its interaction with other elements, requires further investigation [90]. The accumulation of Na in otoliths may indicate contamination, as sodium can be incorporated after fish capture, during dissection or otolith preparation [91]. Unlike other elements, such as strontium (Sr) and calcium (Ca), Na does not bind strongly to otolith crystals and can diffuse depending on the liquid in which the otolith is immersed. This behavior makes Na less useful for stock discrimination and for inferring the environment inhabited by the fish [91]. Thus, the cause of the difference between the regions is unclear. One hypothesis for the lower values in the center region compared to the other two regions is that it is an area with a more extensive continental shelf, which may reduce the influence of anthropogenic contamination.

Although regional differences are somewhat evident in the univariate tests for some shape and elemental predictors, the combined use of the otolith contour and chemical signatures reinforces the idea that *U. cirrata* operates as a connected single population-unit. In addition to the elements that showed significant regional differences, the uniform concentrations of Mn, Co, Se, Li, and Rb across regions, combined with overlapping shape traits, further support this idea. Studies on congeneric species, such as *U. brasiliensis* [31], and other Gadiforms, such as *Merluccius hubbsi* [92], have documented similar patterns, where regional variations reflect environmental influences without a clear population segregation.

The integration of the otolith shape and elemental analyses revealed that, although the *U. cirrata* population is predominantly connected, it is partially influenced by regional environmental factors, such as water chemistry, prey availability, and habitat characteristics. These influences can be observed in significant regional variations in otolith elemental composition profiles, such as differences in the concentrations of elements such as Na, Sr, Mg, Ba, and As, which are directly linked to environmental characteristics such as salinity, temperature, and nutrient availability [56,93]. While Mn, Co, Se, Li, and Rb remain consistent across regions, their stability highlights a baseline of population connectivity, contrasting with the localized environmental drivers of variability in other elements.

The interaction between water masses, water chemistry, and food availability across regions influences the incorporation of elements into otoliths, reflecting local ecological dynamics [48,68]. Furthermore, ontogenetic factors, such as age and developmental stage, also play an important role in the bioaccumulation of certain elements, such as arsenic, which varies according to environmental conditions and diet availability in each region [80]. This aligns with findings in *U. brasiliensis* and the Mediterranean hake (*Merluccius merluccius*), where environmental gradients shape population patterns without creating strict segregation [94]. Such results further reinforce the role of environmental and ecological processes in shaping the spatial population structure of *U. cirrata*.

5. Conclusions

This study confirms significant regional variations in the otolith morphology and chemical composition of *Urophycis cirrata*, reflecting the influence of environmental factors on the species' population structure. Multivariate analysis revealed regional differentiation, but the overlap in otolith data suggests a largely connected population. Local environmental factors, such as water chemistry, prey availability, and habitat characteristics, influence the population structure, despite this connectivity.

For fisheries management, it is important to consider regional variations, even though *U. cirrata* can be treated as a single population. Incorporating strategies, such as fishing

exclusion zones and regional catch limits, can help ensure the population's sustainability in the Southwestern Atlantic.

Finally, future research should integrate techniques such as population genetics and otolith isotopic analysis, along with more extensive temporal datasets, to examine interannual variations and assess climate change impacts.

Author Contributions: C.S.: Methodology, Investigation, Formal analysis, Writing—original draft. C.L.D.B.R.-W.: Supervision, Project administration. A.R.: Methodology, Formal Analysis. A.A.: Resources. E.P.: Methodology. A.T.C.: Supervision, Project administration, Methodology, Formal Analysis, Conceptualization, Financial Support, Writing—Review and Editing. All authors have read and agreed to the published version of the manuscript.

Funding: This study was funded by national resources through the Foundation for Science and Technology (FCT) under the framework of projects UIDB/04423/2020 and UIDP/04423/2020. Sincere thanks to the Coordination for the Improvement of Higher Education Personnel (CAPES) for granting a doctoral scholarship to the first author and to PDSE-CAPES (88881.982432/2024-01) for supporting the Sandwich Doctorate Abroad scholarship.

Informed Consent Statement: Not applicable.

Data Availability Statement: Data could be shared upon request.

Acknowledgments: We thanks Marcelo Roberto Souto de Melo and Pollyana Roque for their timely assistance.

Conflicts of Interest: The authors declare no conflicts of interest.

References

1. Cohen, D.M.; Inada, T.; Iwamoto, T.; Scialabba, N. *FAO Species Catalogue Vol 10 Gadiform Fishes of the World (Order Gadiformes) an Annotated Illustrated Catalogue of Cods Hakes Grenadiers Other Gadiform Fishes Known to Date*; FAO: Rome, Italy, 1990.
2. Menezes, N.A.; Buckup, P.A.; de Figueiredo, J.L.; de Moura, R.L. (Eds.) *Catálogo das Espécies de Peixes Marinhos do Brasil*; Museu de Zoologia da Universidade de São Paulo: São Paulo, Brasil, 2003; Volume 1.
3. Melo, M.R.S.; Braga, A.C.G.; Nunan, W.A.; Costa, P.A.S. On new collections of deep-sea Gadiformes (Actinopterygii: Teleostei) from the Brazilian continental slope, between 11° and 23°S. *Zootaxa* **2010**, *2433*, 25–46. [CrossRef]
4. Lemes, P.C.R.; Melo, M.R.S. Phycidae in Catálogo Taxonômico da Fauna do Brasil. Available online: http://fauna.jbrj.gov.br/fauna/faunadobrasil/40479 (accessed on 29 December 2024).
5. Cousseau, M.B. Las especies del orden gadiformes del Atlántico sudamericano comprendido entre 34° y 55° y su relación con las de otras áreas. *Frente Marít.* **1993**, *13*, 7–102.
6. Lemes, P.C.R. Revisão taxonômica das abróteas do gênero *Urophycis* Gill, 1863 no Atlântico Sul (Gadiformes: Gadidae). Master's Dissertation, Universidade de São Paulo, São Paulo, Brazil, 2017.
7. Martins, R.S.; Haimovici, M. Determinação de idade, crescimento e longevidade da abrótea de profundidade, *Urophycis cirrata*, Goode & Bean, 1896, (Teleostei: Phycidae) no extremo sul do Brasil. *Atântica* **2000**, *22*, 57–70.
8. Balbi, T.J.; Wongtschowski, C.L.D.B.R.; Santificetur, C. Growth of the Brazilian codling, *Urophycis mystacea* (Phycidae-Gadiformes) of southeastern Brazil. *Bol. Inst. Pesca.* **2019**, *45*, 1–7. [CrossRef]
9. Bernardes, R.A.; Figueiredo, J.L.; Rodrigues, A.; Fischer, L.G.; Vooren, C.M.; Haimovici, M.; Rossi-Wongtschowski, C.L.D.B. *Peixes da Zona Econômica Exclusiva da Região Sudeste do Brasil. Levantamento com Armadilhas, Pargueiras e Redes de Arrasto de Fundo*; Series Documentos REVIZEE; Editora da Universidade de São Paulo: São Paulo, Brasil, 2005.
10. Haimovici, M.; Ávila-da-Silva, A.O.; Rossi-Wongtschowski, C.L.D.B. *Prospecção Pesqueira de Espécies Demersais com Espinhel de Fundo na Zona Econômica*; Series Documentos REVIZEE; Editora da Universidade de São Paulo: São Paulo, Brasil, 2004.
11. Dery, L.M. Red hake, Urophycis chuss. In *Age Determination Methods for Northwest Atlantic Species*; Pentilla, J., Dery, L.M., Eds.; NOAA Technical Report NMFS 72; National Marine Fisheries Service: Silver Spring, MD, USA, 1988; pp. 49–58.
12. Casas, J.M.; Piñeiro, C. Growth and age estimation of greater fork-beard (Phycis blennoides Brünnich, 1768) in the north and northwest of the Iberian Peninsula (ICES division VIIIc and IXa). *Fish. Res.* **2000**, *47*, 19–25. [CrossRef]
13. Matic-Skoko, J.; Ferri, J.; Skeljo, F.; Bartulovic, V.; Glavic, K.; Glamuzina, B. Age, growth and validation of otolith morphometrics as predictors of age in the forkbeard, Phycis phycis (Gadidae). *Fish. Res.* **2011**, *112*, 52–58. [CrossRef]

14. Haimovici, M.; Ávila-da-Silva, A.O.; Fischer, L.G. Diagnóstico do estoque e orientações para o ordenamento da pesca de Urophycis mystacea (Ribeiro, 1903). In *Análise das Principais Pescarias Comerciais da Região Sudeste-Sul do Brasil: Dinâmica Populacional das Espécies em Exploração—II*; Rossi-Wongtschowski, C.L.D.B., Ávila-da-Silva, A.O., Cergole, M.C., Eds.; Series Documentos REVIZEE; Editora da Universidade de São Paulo: São Paulo, Brasil, 2006; pp. 86–94.
15. Haimovici, M.; Rossi-Wongtschowski, C.L.D.B.; Bernardes, R.A.; Fisher, L.G.; Vooren, C.M.; Santos, R.A.; Rodrigues, A.R. *Santos S 2008 Prospecção Pesqueira de Espécies Demersais com Rede de Arrasto-Defundo na Região Sudeste-Sul do Brasil*; Series Documentos REVIZEE; Editora da Universidade de São Paulo: São Paulo, Brasil, 2008.
16. Haimovici, M.; Martins, A.S.; Figueiredo, J.L.; Vieira, P.C. Demersal bony fish of the outer shelf and upper slope of the southern Brazil Subtropical Convergence Ecosystem. *Mar. Ecol. Prog. Ser.* **1994**, *108*, 59–77. [CrossRef]
17. Perez, J.A.A.; Pezzuto, P.; Wahrlich, R.; Soares, A.L.S. Deep-water fisheries in Brazil: History, status, and perspectives. *Lat. Am. J. Aquat. Res.* **2009**, *37*, 513–541. [CrossRef]
18. Trindade-Santos, I.; Freire, K.M.F. Analysis of reproductive patterns of fishes from three large marine ecosystems. *Front. Mar. Sci.* **2015**, *2*, 38. [CrossRef]
19. Pio, V.M.; Pezzuto, P.R.; Wahrlich, R. Only two fisheries? Characteristics of the industrial bottom gillnet fisheries in southeastern and southern Brazil and their implications for management. *Lat. Am. J. Aquat. Res.* **2016**, *44*, 882–897.
20. Oceana. Auditoria da Pesca Brasil 2023. 2023. Available online: https://brasil.oceana.org/wp-content/uploads/sites/23/Apendice-2-Estoques-Pesqueiros-2021_Final-1.pdf (accessed on 29 December 2024).
21. Panfili, J.; de Pontual, H.; Troadec, H.; Wright, P.J. Otoliths: A tool for monitoring the environment. Developments in Aquac. *Fish. Sci.* **2002**, *36*, 123–150.
22. Correia, A.T.; Moura, A.; Triay-Portella, R.; Santos, P.T.; Pinto, E.; Almeida, A.A.; Sial, A.N.; Muniz, A.A. Population structure of the chub mackerel (*Scomber colias*) in the NE Atlantic inferred from otolith elemental and isotopic signatures. *Fish. Res.* **2021**, *234*, 105785. [CrossRef]
23. de Almeida PR, C.; da Costa, M.R.; Ribeiro AT, R.; Almeida, A.; Azevedo, R.; Monteiro-Neto, C.; Correia, A.T. Population structure and habitat connectivity of *Pogonias courbina* (Perciformes, Sciaenidae) in two Brazilian lagoon systems on south-east coast of Rio de Janeiro, Brazil, inferred from otolith shape and elemental signatures. *J. Sea Res.* **2024**, *199*, 102500. [CrossRef]
24. Izzo, C.; Reis-Santos, P.; Gillanders, B.M. Otolith chemistry: Principles and applications in fishery science. *Fish. Res.* **2018**, *208*, 160–175. [CrossRef]
25. Reis-Santos, P.; Tanner, S.E.; Vasconcelos, R.P.; Elsdon, T.S.; Cabral, H.N.; Gillanders, B.M. Connectivity between estuarine and coastal fish populations: Contributions of estuaries are not consistent over time. *Mar. Ecol. Prog. Ser.* **2013**, *491*, 177–186. [CrossRef]
26. Santos, J.F.; Moreira, M.E.; Correia, A.T. Morphological variability in fish otoliths and its ecological implications. *Mar. Ecol. Prog. Ser.* **2017**, *580*, 123–134.
27. Schroeder, R.; Schwingel, P.R.; Pinto, E.; Almeida, A.; Correia, A.T. Stock structure of the Brazilian sardine *Sardinella brasiliensis* from Southwest Atlantic Ocean inferred from otolith elemental signatures. *Fish. Res.* **2022**, *248*, 106192. [CrossRef]
28. Daros, F.A.; Spach, H.L.; Sial, A.N.; Correia, A.T. Otolith fingerprints of the coral reef fish *Stegastes fuscus* in southeast Brazil: A useful tool for population and connectivity studies. *Reg. Stud. Mar. Sci.* **2016**, *3*, 262–272. [CrossRef]
29. Adelir-Alves, J.; Daros, F.A.; Spach, H.L.; Soeth, M.; Correia, A.T. Otoliths as a tool to study reef fish population structure from coastal islands of South Brazil. *Mar. Biol. Res.* **2018**, *14*, 973–988. [CrossRef]
30. Soeth, M.; Spach, H.L.; Daros, F.A.; Adelir-Alves, J.; Almeida AC, O.; Correia, A.T. Stock structure of Atlantic Spadefish *Chaetodipterus faber* from Southwest Atlantic Ocean inferred from otolith elemental and shape signatures. *Fish. Res.* **2018**, *211*, 81–90. [CrossRef]
31. Biolé, F.G.; Thompson, G.A.; Vargas, C.V.; Leisen, M.; Barra, F.; Volpedo, A.V.; Avigliano, E. Fish stocks of *Urophycis brasiliensis* revealed by otolith fingerprint and shape in the Southwestern Atlantic Ocean. *Coast. Mar. Sci.* **2018**, *229*, 106406. [CrossRef]
32. Figueiredo, J.L.; Menezes, N.A. *Manuel dos Peixes Marinhos do Sudeste do Brasil. Vol (II): Teleostei (1)*; Museu de Zoologia da Universidade de São Paul: São Paulo, Brasil, 1978; pp. 44–45.
33. Madureira, L.S.P.; Rossi-Wongtschowski, C.L.D.B. (Eds.) *Prospecção de Recursos Pesqueiros Pelágicos na Zona Econômica Exclusiva da Região Sudeste-Sul do Brasil: Hidroacústica e Biomassas*; Series Documentos REVIZEE; Editora da Universidade de São Paulo: São Paulo, Brasil, 2005.
34. Iwata, H.; Ukai, Y. SHAPE: Um pacote de programa de computador para avaliação quantitativa de formas biológicas baseada em descritores de Fourier elípticos. *J. Hered.* **2002**, *93*, 384–385. [CrossRef] [PubMed]
35. Ferguson, G.J.; Ward, T.M.; Gillanders, B.M. Otolith shape and elemental composition: Complementary tools for stock discrimination of mulloway (*Argyrosomus japonicus*) in southern Australia. *Fish. Res.* **2011**, *110*, 75–83. [CrossRef]
36. Kuhl, F.P.; Giardina, C.R. Elliptic Fourier features of a closed contour. *Comput. Graph. Image Process.* **1982**, *18*, 236–258. [CrossRef]
37. Rooker, J.; Zdanowicz, V.; Secor, D. Chemistry of tuna otoliths: Assessment of base composition and postmortem handling effects. *Mar. Biol.* **2001**, *139*, 35–43. [CrossRef]

38. Patterson, H.M.; Thorrold, S.R.; Shenker, J.M. Analysis of otolith chemistry in Nassau grouper (*Epinephelus striatus*) from the Bahamas and Belize using solution-based ICP-MS. *Coral Reefs* **1999**, *18*, 171–178. [CrossRef]
39. Sturgeon, R.E.; Willie, S.N.; Yang, L.; Greenberg, R.; Spatz, R.O.; Chen, Z.; Scriver, C.; Clancy, V.; Lam, J.W.; Thorrold, S. Certification of a fish otolith reference material in support of quality assurance for trace element analysis. *J. Anal. At. Spectrom.* **2005**, *20*, 1067–1071. [CrossRef]
40. Higgins, R.; Isidro, E.; Menezes, G.; Correia, A. Otolith elemental signatures indicate population separation in deep-sea rockfish, Helicolenus dactylopterus and Pontinus kuhlii, from the Azores. *J. Sea. Res.* **2013**, *83*, 202–208. [CrossRef]
41. de Almeida PR, C.; da Costa, M.R.; de Oliveira RS, C.; Almeida, A.; Azevedo, R.; Monteiro-Neto, C.; Correia, A.T. The use of the shape and chemistry of fish otoliths as a subpopulational discrimination tool for Eugerres brasilianus in lagoon systems in the Southwest Atlantic Ocean. *Fish. Res.* **2023**, *267*, 106795. [CrossRef]
42. Campana, S.E.; Chouinard, G.A.; Hanson, J.M.; Frechet, A.; Brattey, J. Otolith elemental fingerprints as biological tracers of fish stocks. *Fish. Res.* **2000**, *46*, 343–357. [CrossRef]
43. Correia, A.T.; Hamer, P.; Carocinho, B.; Silva, A. Evidence for meta-population structure of *Sardina pilchardus* in the Atlantic Iberian waters from otolith elemental signatures of a strong cohort. *Fish. Res.* **2014**, *149*, 76–85. [CrossRef]
44. Vaz-dos-Santos, A.M.; Rautenberg, K.A.; Augusto, C.G.; Ballester, E.L.C.; Schwingel, P.R.; Pinto, E.; Almeida, A.; Correia, A.T. Geographic variation in *Opisthonema oglinum* (Lesueur, 1818) in the southeastern Brazilian Bight inferred from otolith shape and chemical signatures. *Fishes* **2023**, *8*, 234. [CrossRef]
45. de Almeida, P.R.C.; Rodrigues da Costa, M.; Dias de Souza Coutinho, R.; Méndez-Vicente, A.; Pisonero Castro, J.; Monteiro-Neto, C.; de Almeida Tubino, R.; Correia, A.T. Use of otolith microchemistry signatures to assess the habitat use of *Centropomus undecimalis* in lagoon systems of the southwest Atlantic. *Reg. Stud. Mar. Sci.* **2024**, *73*, 103470. [CrossRef]
46. Brandini, F.P.; Tura, P.M.; Santos, P.P. Ecosystem responses to biogeochemical fronts in the South Brazil Bight. *Progr. Oceanogr.* **2018**, *164*, 52–62. [CrossRef]
47. da Silveira, I.C.A.; Napolitano, D.C.; Farias, I.U. Water Masses and Oceanic Circulation of the Brazilian Continental Margin and Adjacent Abyssal Plain. In *Brazilian Deep-Sea Biodiversity*; Sumida, P.Y.G., Bernardino, A.F., De Léo, F.C., Eds.; Springer: Cham, Switzerland, 2020.
48. Piola, A.R.; Campos, E.J.; Möller, O.O., Jr.; Charo, M.; Martinez, C. Subtropical shelf front off eastern South America. *J. Geophys. Res. Ocean.* **2000**, *105*, 6565–6578. [CrossRef]
49. Campos, E.J.; Mulkherjee, S.; Piola, A.R.; de Carvalho, F.M. A note on a mineralogical analysis of the sediments associated with the Plata River and Patos Lagoon outflows. *Cont. Shelf Res.* **2000**, *28*, 1687–1691. [CrossRef]
50. Mahiques, M.M.; Tessler, M.G.; Ciotti, A.M.; da Silveira IC, A.; Sousa SH, D.M.; Figueira RC, L.; Tassinari, C.C.G.; Furtado, V.V.; Passos, R.F. Hydrodynamically driven patterns of recent sedimentation in the shelf and upper slope off Southeast Brazil. *Cont. Shelf Res.* **2004**, *24*, 1685–1697. [CrossRef]
51. Nagai, R.; Ferreira, P.; Mulkherjee, S.; Martins, M.; Figueira, R.; Sousa, S.; Mahiques, M. Hydrodynamic controls on the distribution of surface sediments from the southeast South American continental shelf between 23 S and 38 S. *Cont. Shelf Res.* **2014**, *89*, 51–60. [CrossRef]
52. Galley, E.A.; Wright, P.J.; Gibb, F.M. Combined methods of otolith shape analysis improve identification of spawning areas of Atlantic cod. *ICES J. Mar. Sci.* **2006**, *63*, 1710–1717. [CrossRef]
53. Stransky, C.; Murta, A.G.; Schlickeisen, J.; Zimmermann, C. Otolith shape analysis as a tool for stock separation of horse mackerel (*Trachurus trachurus*) in the Northeast Atlantic and Mediterranean. *Fish. Res.* **2008**, *89*, 159–166. [CrossRef]
54. Hoff, N.T.; Dias, J.F.; Pinto, E.; Almeida, A.; Schroeder, R.; Correia, A.T. Past and contemporaneous otolith fingerprints reveal potential anthropogenic interferences and allows refinement of the population structure of *Isopisthus parvipinnis* in the South Brazil Bight. *Biology* **2022**, *11*, 1005. [CrossRef] [PubMed]
55. Santificetur, C.; Rossi-Wongtschowski, C.L.D. Sagittae otolith's morphometry as a tool for analysis of population structure of the *Urophycis mystacea* Ribeiro, 1903 (Teleostei: Phycidae) from the Southeastern-Southern Brazil. *Front. Mar. Sci.* **2016**, *3*, 221. [CrossRef]
56. Moreira, C.; Froufe, E.; Sial, A.N.; Caeiro, A.; Vaz-Pires, P.; Correia, A.T. Population structure of the blue jack mackerel (*Trachurus picturatus*) in the NE Atlantic inferred from otolith microchemistry. *Fish. Res.* **2018**, *197*, 113–122. [CrossRef]
57. Thomas, O.R.B.; Swearer, S.E. Otolith Biochemistry—A Review. *Rev. Fish. Sci. Aquac.* **2019**, *27*, 458–489. [CrossRef]
58. Campana, S.E. Chemistry and composition of fish otoliths: Pathways, mechanisms and applications. *Mar. Ecol. Prog. Ser.* **1999**, *188*, 263–297. [CrossRef]
59. Sturrock, A.M.; Hunter, E.; Milton, J.A.; Eimf; Johnson, R.C.; Waring, C.P.; Trueman, C.N.; Eimf, E. Quantifying physiological influences on otolith microchemistry. *Methods Ecol. Evol.* **2015**, *6*, 806–816. [CrossRef]
60. Hüssy, K.; Limburg, K.E.; De Pontual, H.; Thomas, O.R.; Cook, P.K.; Heimbrand, Y.; Blass, M.; Sturrock, A.M. Trace element patterns in otoliths: The role of biomineralization. *Rev. Fish. Sci. Aquac.* **2021**, *29*, 445–477. [CrossRef]

61. Albuquerque, C.Q. Los otolitos como indicadores del ciclo de vida, de patrones poblacionales, y del uso y características ambientales de los ecosistemas. In *Métodos de Estudios con Otolitos: Principios y Aplicaciones*; Volpedo, A.V., Vaz-dos-Santos, A.M., Eds.; CAFP-PIESCI: Buenos Aires, Argentina, 2015; pp. 139–166.
62. Miller, M.B.; Clough, A.M.; Batson, J.N.; Vachet, R.W. Transition metal binding to cod otolith proteins. *J. Exp. Mar. Bio. Ecol.* **2006**, *329*, 135–143. [CrossRef]
63. Elsdon, T.S.; Wells, B.K.; Campana, S.E.; Gillanders, B.M.; Jones, C.M.; Limburg, K.E.; Secor, D.H.; Thorrold, S.R.; Walther, B.D. Otolith chemistry to describe movements and life-history parameters of fishes: Hypotheses, assumptions, limitations, and inferences. *Oceanogr. Mar. Biol.* **2008**, *46*, 297–330.
64. He, S.; Xu, Y.J. Spatiotemporal distributions of Sr and Ba along an estuarine river with a large salinity gradient to the Gulf of Mexico. *Water* **2016**, *8*, 323. [CrossRef]
65. Soeth, M.; Spach, H.L.; Daros, F.A.; Castro, J.P.; Correia, A.T. Use of otolith elemental signatures to unravel lifetime movement patterns of Atlantic spadefish, *Chaetodipterus faber*, in the Southwest Atlantic Ocean. *J. Sea Res.* **2020**, *158*, 101873. [CrossRef]
66. Moreira, C.; Froufe, E.; Vaz-Pires, P.; Triay-Portella, R.; Méndez, A.; Castro, J.P.; Correia, A.T. Unravelling the spatial-temporal population structure of *Trachurus picturatus* across the North-East Atlantic using otolith fingerprinting. *Coast. Mar. Sci.* **2022**, *272*, 107860. [CrossRef]
67. Peterson, R.G.; Stramma, L. Upper-level circulation in the South Atlantic Ocean. *Prog. Oceanogr.* **1991**, *26*, 1–73. [CrossRef]
68. Stramma, L.; England, M. On the water masses and mean circulation of the South Atlantic Ocean. *J. Geophys. Res. Ocean.* **1999**, *104*, 20863–20883. [CrossRef]
69. Tomczak, M.; Godfrey, J.S. *Regional Oceanography: An Introduction*; Daya Books: New Delhi, India, 2003.
70. Elsdon, T.S.; Gillanders, B.M. Identifying migratory contingents of fish by combining otolith Sr: Ca with temporal collections of ambient Sr: Ca concentrations. *J. Fish Biol.* **2006**, *69*, 643–657. [CrossRef]
71. Hamer, P.A.; Jenkins, G.P. Comparison of spatial variation in otolith chemistry of two fish species and relationships with water chemistry and otolith growth. *J. Fish Biol.* **2007**, *71*, 1035–1055. [CrossRef]
72. Barnes, T.C.; Gillanders, B.M. Combined effects of extrinsic and intrinsic factors on otolith chemistry: Implications for environmental reconstructions. *Can. J. Fish. Aquat. Sci.* **2013**, *70*, 1159–1166. [CrossRef]
73. Thomas, O.R.; Thomas, K.V.; Jenkins, G.P.; Swearer, S.E. Spatio-temporal resolution of spawning and larval nursery habitats using otolith microchemistry is element dependent. *Mar. Ecol. Prog. Ser.* **2020**, *636*, 169–187. [CrossRef]
74. Schenone, N.F.; Volpedo, A.V.; Cirelli, A.F. Trace metal contents in water and sediments in Samborombón Bay wetland, Argentina. *Wetl. Ecol. Manag.* **2007**, *15*, 303–310. [CrossRef]
75. Rosso, J.J.; Schenone, N.F.; Pérez Carrera, A.; Fernández Cirelli, A. Concentration of arsenic in water, sediments and fish species from naturally contaminated rivers. *Environ. Geochem. Health* **2013**, *35*, 201–214. [CrossRef] [PubMed]
76. Avigliano, E.; Schenone, N.F. Human health risk assessment and environmental distribution of trace elements, glyphosate, fecal coliform, and total coliform in Atlantic rainforest mountain rivers (South America). *Microchem. J.* **2015**, *122*, 149–158. [CrossRef]
77. Angeli JL, F.; Trevizani, T.H.; Ribeiro, A.; Machado ED, C.; Figueira RC, L.; Markert, B.; Fraenzie, S.; Wuenschmann, S. Arsenic and other trace elements in two catfish species from Paranaguá Estuarine Complex, Paraná, Brazil. *Environ. Monit. Assess.* **2013**, *185*, 8333–8342. [CrossRef]
78. Avigliano, E.; Lozano, C.; Plá, R.R.; Volpedo, A.V. Toxic element determination in fish from Paraná River Delta (Argentina) by neutron activation analysis: Tissue distribution and accumulation and health risk assessment by direct consumption. *J. Food Compos. Anal.* **2016**, *54*, 27–36. [CrossRef]
79. Gao, Y.; Baisch, P.; Mirlean, N.; Rodrigues da Silva Júnior, F.M.; van Larebeke, N.; Baeyens, W.; Leermakers, M. Arsenic speciation in fish and shellfish from the North Sea (southern bight) and Acu port area (Brazil) and health risks related to seafood consumption. *Chemosphere* **2018**, *191*, 89–96. [CrossRef] [PubMed]
80. Erickson, R.J.; Mount, D.R.; Highland, T.L.; Hockett, J.R.; Jenson, C.T. The relative importance of waterborne and dietborne arsenic exposure on survival and growth of juvenile rainbow trout. *Aquat. Toxicol.* **2011**, *104*, 108–115. [CrossRef] [PubMed]
81. Has-Schön, E.; Bogut, I.; Vuković, R.; Galović, D.; Bogut, A.; Horvatić, J. Distribution and age-related bioaccumulation of lead (Pb), mercury (Hg), cadmium (Cd), and arsenic (As) in tissues of common carp (*Cyprinus carpio*) and European catfish (*Sylurus glanis*) from the Buško Blato reservoir (Bosnia and Herzegovina). *Chemosphere* **2015**, *135*, 289–296. [CrossRef]
82. Bubach, D.F.; Catán, S.P.; Baez, V.H.; Arribére, M.A. Elemental composition in rainbow trout tissues from a fish farm in Patagonia, Argentina. *Environ. Sci. Pollut. Res.* **2018**, *25*, 6340–6351. [CrossRef]
83. Grammer, G.L.; Morrongiello, J.R.; Izzo, C.; Hawthorne, P.J.; Middleton, J.F.; Gillanders, B.M. Coupling biogeochemical tracers with fish growth reveals physiological and environmental controls on otolith chemistry. *Ecol. Monogr.* **2017**, *87*, 487–507. [CrossRef]
84. Halden, N.M.; Friedrich, L.A. Trace-element distributions in fish otoliths: Natural markers of life histories, environmental conditions and exposure to tailings effluence. *Mineral. Magazine.* **2008**, *72*, 593–605. [CrossRef]

85. Daros, F.A.; Condini, M.V.; Altafin, J.P.; de Oliveira Ferreira, F.; Hostim-Silva, M. Fish otolith microchemistry as a biomarker of the world's largest mining disaster. *Sci. Total Environ.* **2022**, *807*, 151780. [CrossRef]
86. Begg, G.A.; Cappo, M.; Cameron, D.S.; Boyle, S.; Sellin, M.J. Stock discrimination of school mackerel, *Scomberomorus queenslandicus*, and spotted mackerel, *Scomberomorus munroi*, in coastal waters of eastern Australia by analysis of minor and trace elements in whole otoliths. *Fish. Bull.* **1998**, *96*, 653–666.
87. Mohan, J.; Rahman, M.S.; Thomas, P.; Walther, B. Influence of constant and periodic experimental hypoxic stress on Atlantic croaker otolith chemistry. *Aquat. Biol.* **2014**, *20*, 1–11. [CrossRef]
88. Hoff, G.R.; Fuiman, L.A. Environmentally induced variation in elemental composition of red drum (*Sciaenops ocellatus*) otoliths. *Bull. Mar. Sci.* **1995**, *56*, 578–591.
89. Gao, Y.; Feng, Q.; Ren, D.; Qiao, L.; Li, S. The relationship between trace elements in fish otoliths of wild carp and hydrochemical conditions. *Fish. Physiol. Biochem.* **2010**, *36*, 91–100. [CrossRef] [PubMed]
90. Payan, P.; Edeyer, A.; de Pontual, H.; Borelli, G.; Boeuf, G.; Mayer-Gostan, N. Chemical composition of saccular endolymph and otolith in fish inner ear: Lack of spatial uniformity. *Am. J. Physiol. Regul. Integr. Comp. Physiol.* **1999**, *277*, R123–R131. [CrossRef] [PubMed]
91. Tomás, J.; Geffen, A.J.; Millner, R.S.; Pineiro, C.G.; Tserpes, G. Elemental composition of otolith growth marks in three geographically separated populations of European hake (*Merluccius merluccius*). *Mar. Biol.* **2006**, *148*, 1399–1413. [CrossRef]
92. Vaz-Dos-Santos, A.M.; dos Santos-Cruz, N.N.; de Souza, D.; Giombelli-Da-Silva, A.; Gris, B.; Rossi-Wongtschowski, C.L.D.B. Otoliths sagittae of *Merluccius hubbsi*: An efficient tool for the differentiation of stocks in the Southwestern Atlantic. *Braz. J. Oceanogr.* **2017**, *65*, 520–525. [CrossRef]
93. Sturrock, A.M.; Trueman, C.N.; Darnaude, A.M.; Hunter, E. Can otolith elemental chemistry retrospectively track migrations in fully marine fishes? *J. Fish Biol.* **2012**, *81*, 766–795. [CrossRef]
94. Morales-Nin, B.; Pérez-Mayol, S.; MacKenzie, K.; Catalán, I.A.; Palmer, M.; Kersaudy, T.; Mahé, K. European hake (*Merluccius merluccius*) stock structure in the Mediterranean as assessed by otolith shape and microchemistry. *Fish. Res.* **2022**, *254*, 106419. [CrossRef]